Supporting Information

A mesoporous polydopamine nanoparticle enables highly efficient manganese encapsulation for enhanced MRI-guided photothermal therapy

Yan Wu,[a] Yu Huang,[a] Chunlai Tu,[a] Fengren Wu,[a] Gangsheng Tong,[a] Yue Su,[a,b,c] Li Xu,[a,b,c] Xiaoqin Zhang,*[b,c] Shuqiang Xiong,*[a] Xinyuan Zhu[a]*

[a] School of Chemistry and Chemical Engineering, Frontiers Science Center for Transformative Molecules, Shanghai Jiao Tong University, 800 Dongchuan Road, Shanghai 200240, China.

b Fengxian Hospital affiliated to Southern Medical University, 6600 Nanfeng Road, Shanghai 201499, P.R.China.

c Southern Hospital of Sixth People's Hospital affiliated to Shanghai Jiao Tong University, 6600 Nanfeng Road, Shanghai 201499, P.R.China.

**Corresponding authors. E-mail: alicexu@sjtu.edu.cn (L. Xu), zxq217@smu.edu.cn (X. Zhang), xsq123@sjtu.edu.cn (S. Xiong)*

KEYWORDS: theranostic nanoplatform, mesoporous polydopamine nanoparticles, highly loaded manganese, superior MRI effect, enhanced photothermal cancer therapy

Materials

Methyl thiazolyl tetrazolium (MTT) and calcein acetoxymethyl ester (Calcein-AM) were purchased from Sigma-Aldrich Co. Ltd. Dulbecco's Modified Eagle Medium (DMEM), fetal bovine serum (FBS) and Alexa fluor®488 annexin V kit were supplied by Thermo Fisher Co. Ltd.

Synthesis and characterization

Zeta potential and dynamic light scattering (DLS) were measured by a Zatasizer Nanoseries ZS (Malvern, UK). The contents of Mn element were determined by TGA (Pyris 1, USA) and inductively coupled plasma mass spectrometer (ICP-MS, iCAP Q, USA). The specific surface areas and pore size of the nanoparticles were measured through a surface area and porosity analyzer (Autosorb-IQ3, USA) and calculated by the methods of Brunauer-Emmett-Teller (BET) and Barrett-Joyner-Halenda (BJH). The stability of Mn^{2+} on nanoparticles was conducted as follows: the dialysis bags containing MPDAPs/Mn and PDAPs/Mn aqueous solutions were immersed into 40 mL of PBS with gently shaken at 37 ºC, separately. At various time points, 2 mL of dialysates were collected to detect the content of Mn by inductive coupled plasma emission spectrometer (ICP) analysis, after which 2 mL of fresh PBS were supplied to maintain the total volume. Furthermore, the UV-vis-NIR absorption spectrums of MPDAPs/Mn and PDAPs/Mn from 200 nm to 1000 nm were recorded by an UV-vis spectrometer (Evolution300, USA).

***In vitro* and *in vivo* T_1-weighted MR imaging**

To determine the corresponding longitudinal relaxivity (r_1) value of $MnCl_2$, PDAPs/Mn, MPDAPs/Mn, a 0.5 T low field MR scanner (MesoMR23-060H-I, Niumag, China) was applied to detect different concentrations of $MnCl_2$, PDAPs/Mn, MPDAPs/Mn in water (the concentrations of Mn^{2+} were 0.4, 0.2, 0.1, 0.05, 0.025 and 0 mM, respectively) at room temperature. For *in vivo* MR Imaging studies, the same MR scanner was employed to take the T_1-weighed images of HeLa tumor-bearing

mice. 9 mice were randomly divided into three groups when the tumors grew up to 1000 ~ 1500 mm^3 (n=3). The mice were anesthetized with 2.5 % isoflurane and injected with 0.2 mL of $MnCl_2$ (0.07 mg/mL), MPDAPs/Mn (1 mg/mL) and PDAPs/Mn (1 mg/mL) through the tail vein. Then the mice were placed into the MR scanner and T_1-weighed images were obtained at the predetermined time points: 0, 1, 4, 8 and 24 h. Scanning parameters: repetition time (TR): 400 ms, echo time (TE): 18.2 ms, field of view (FOV): 100 mm × 100 mm.

***In vitro* and *in vivo* photothermal performance**

To evaluate the photothermal conversion efficiency of the nanoparticles, 1 mL of different concentrations (400, 200, 100, 50, 25, 0 μg/mL) of MPDAPs/Mn or PDAPs/Mn were irradiated with an 808 nm laser at a power density of 2 W/cm^2 for 5 min. During the irradiation, the temperature of the solutions was recorded by a thermal infrared camera (Fluke Ti110, USA). For thermal stability study of the nanoparticles, 1 mL of MPDAPs/Mn or PDAPs/Mn (400 μg/mL) were irradiated with the 808 nm laser and the solutions were allowed to cool down to room temperature for another 10 min, and this procedure was repeated for 5 times. The photothermal conversion efficiency (η) of these nanoparticles were calculated according the Equation S1 and S2 reported previously.[1-2] As for the photothermal conversion efficiency of the nanoparticles *in vivo*, 9 HeLa tumor-bearing mice were randomly divided into 3 groups (n = 3). The 3 groups were injected with 200 μL of PBS, MPDAPs/Mn (1 mg/mL) and PDAPs/Mn (1 mg/mL) *via* the tail vein, respectively. 6 h later, the locations of the tumors were irradiated with 808 nm laser at a density of 2

W/cm^2 for 5 min. The thermal infrared camera was used to take photos and record the temperature changes.

$$\eta = \frac{hS(T_{max}-T_{out})-Q_{dis}}{I(1-10^{-A808})} \quad \text{Equation S1}$$

$$\tau_s = \frac{m_s c_s}{hS} \quad \text{Equation S2}$$

h and S mean the heat transfer coefficient and the surface area of photothermal agents, respectively. T_{Max} and T_{Out} refer to the equilibrium temperature of the solutions and ambient temperature. Q_{Dis} represents the heat dissipation associated with light absorbance of the solution in the container alone. I and $A808$ are the power intensity and absorbance of photothermal agents at 808 nm, respectively. m_S and C_S refer to the mass and heat capacity of aqueous solution.

Cell culture

The mouse fibroblasts cell line (L929) and human cervical cancer cells (HeLa) were cultured with full medium which contains 90 % DMEM and 10% FBS. The temperature and atmosphere were 37 °C and 5 % CO_2, respectively.

***In vitro* cytotoxicity assay**

To investigate the cytotoxicity of different concentrations of MPDAPs/Mn and PDAPs/Mn on L929 cells, a standard MTT assay was conducted. Moreover, calcein-AM was utilized to stain the living cells after irradiation for observing the laser-triggered cell death. HeLa cells were seeded into 6-well plates and next PDAPs/Mn and MPDAPs/Mn (200 μg/mL) were added into the wells followed by laser irradiation. Then, the cells were stained with calcein-AM for 20 min at 37 ºC and

washed with pre-cooled PBS for 3 times. At last, these cells were observed with a fluorescent microscope (Leica, TCS SP8, Germany). For apoptosis analyses by flow cytometry, the cells after irradiation were digested up with trypsin and stained with Alexa fluor®488 annexin V kit. Afterwards, the cells were disposed with BD LSRFortessa flow cytometer.

Animals and tumor models

The BALB/c mice and Sprague-Dawley (SD) rats were purchased from Shanghai Lingchang Company. All animal experiments were operated under the guidance issued by the Institutional Animal Care and Use Committee (IACUC) of Shanghai Jiao Tong University. 2×10^6 HeLa cells in 200 μL PBS were injected into the subcutaneous tissue at right back of each mouse. About 3 weeks later, the tumors approximately grew up to 100 mm^3, and all the mice were divided into five groups (n = 5): PBS, $MnCl_2$, PBS + NIR, PDAPs/Mn + NIR, and MPDAPs/Mn + NIR. The volume of tumor was calculated according to the Equation S3.

$$V=\frac{\text{Length}\times\text{Width}\times\text{Width}}{2} \qquad \text{Equation S3}$$

***In vivo* pharmacokinetics assay**

To study the pharmacokinetics of PDAPs/Mn and MPDAPs/Mn *in vivo*, 6 SD rats (~ 200 g) were randomly divided into 2 groups (n = 3). 1 mL of PDAPs/Mn or MPDAPs/Mn (1 mg/mL) were intravenously administered and 0.5 mL of blood was extracted from the orbit of the SD rats at the predetermined time points: 10 min, 0.5 h, 1 h, 2 h, 4 h, 8 h, 12 h, 24 h. The amount of manganese element in these blood samples were measured by ICP-MS.

Statistical analysis

All the data were presented in terms of standard deviation (mean ± standard, SD). Student's t-test was applied to calculate the differences and $P < 0.05$ means significant difference between the two sets in statistics.

Table S1. ICP-MS Result of PDAPs/Mn and MPDAPs/Mn

Sample	PDAPs/Mn	MDPAPs/Mn
Mean Value	0.903 %	2.764 %
Rep #1	0.908 %	2.753 %
Rep #2	0.905 %	2.768 %
Rep #3	0.897 %	2.772 %

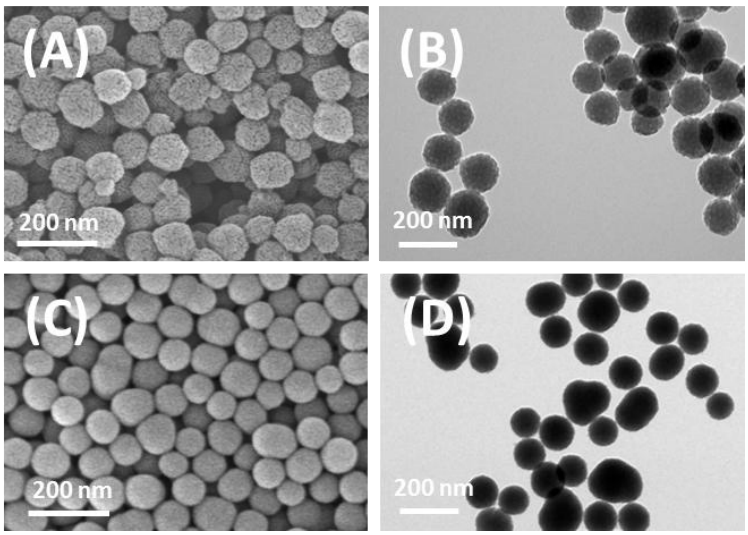

Fig. S1. (A, B) SEM and TEM images of MPDAPs with scale bar of 200 nm, respectively. (C, D) SEM and TEM images of PDAPs with scale bar of 200 nm, respectively.

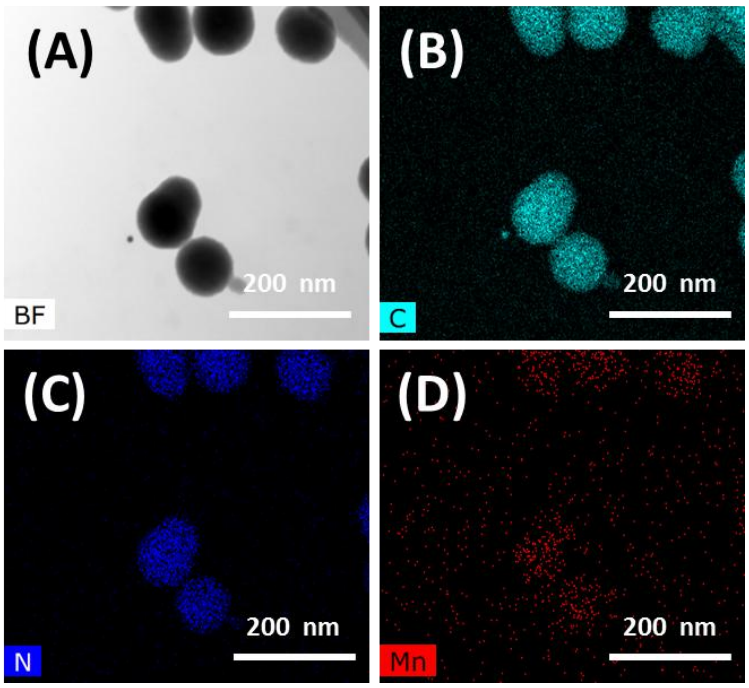

Fig. S2. (A ~ D) HR-TEM mapping of PDAPs/Mn with scale bar of 200 nm.

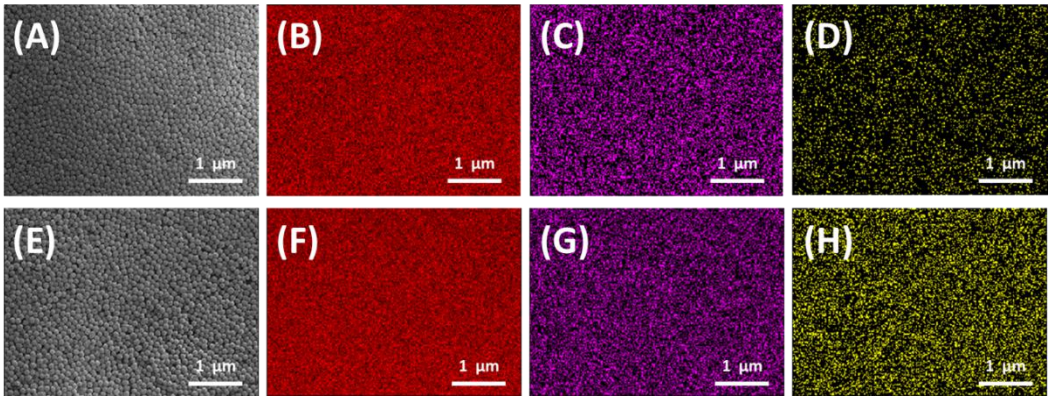

Fig. S3. (A ~ D) SEM mapping images of PDAPs/Mn with scale bar of 1 μm. (E ~ H) SEM mapping images of MPDAPs/Mn with scale bar of 1 μm. Grey means the brief field of the SEM result, red presents the carbon element, purple is the nitrogen element and yellow means the manganese element.

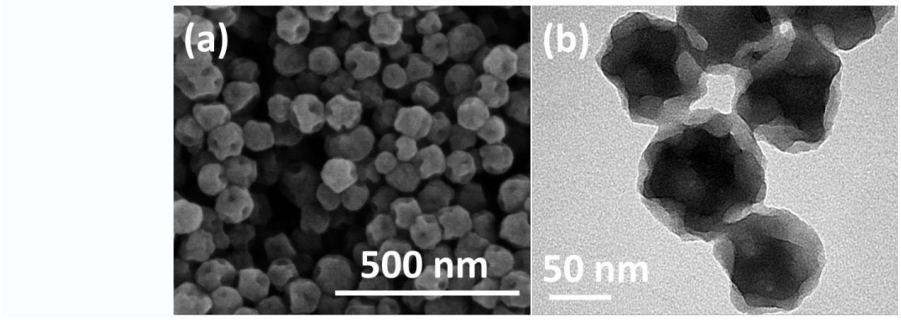

Fig. S4 The mesoporous polydopamine nanoparticles with pore size of about 25 nm.

Table S2. ICP-MS result of MPDAPs/Mn with different pore size

Sample	MDPAPs/Mn (3.4 nm)	MDPAPs-1/Mn (25 nm)
Mean Value	2.764 %	2.472 %
Rep #1	2.753 %	2.478 %
Rep #2	2.768 %	2.468 %
Rep #3	2.772 %	2.470 %

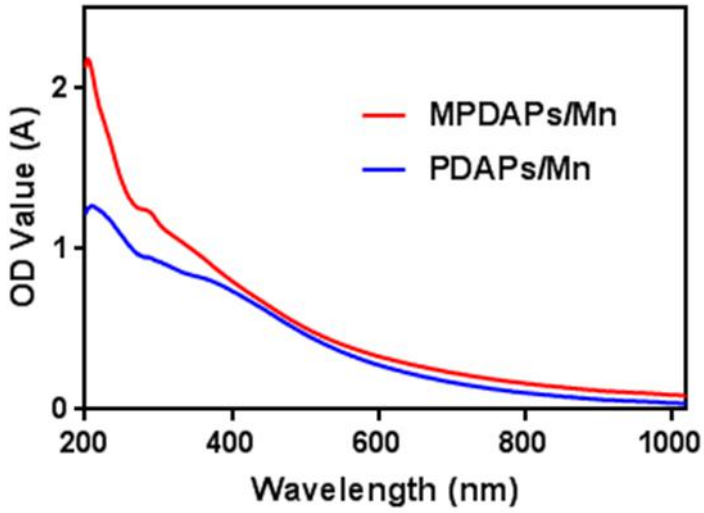

Fig. S5. UV-vis-NIR absorption spectrums (200 nm to 1000 nm) of MPDAPs/Mn and PDAPs/Mn aqueous solution with concentration at 0.01 mg/mL.

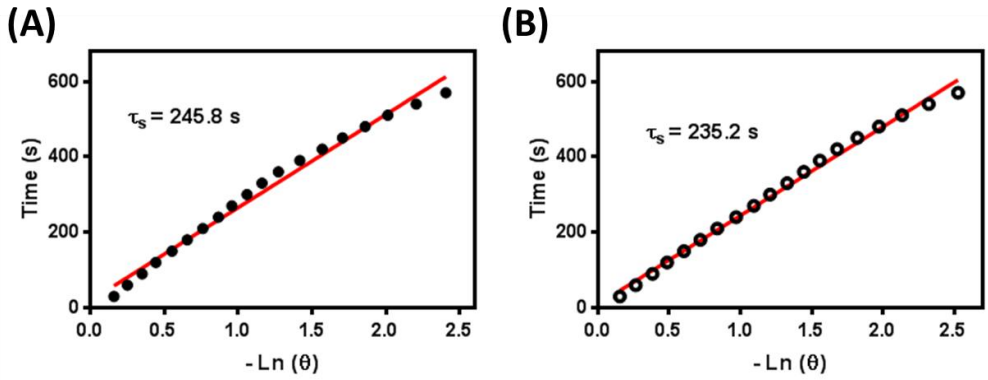

Fig. S6. Plot of cooling time versus–Ln(θ) which is the negative natural logarithm of the temperature driving force from the cooling data in Fig. 2D, (A) is the time constant of PDAPs/Mn and (B) is that of MPDAPs/Mn.

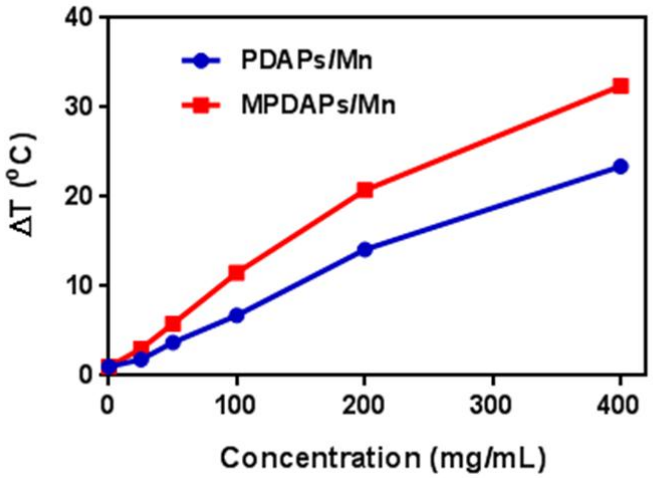

Fig. S7. Plot of temperature change (ΔT) versus different concentrations of MPDAPs/Mn and PDAPs/Mn.

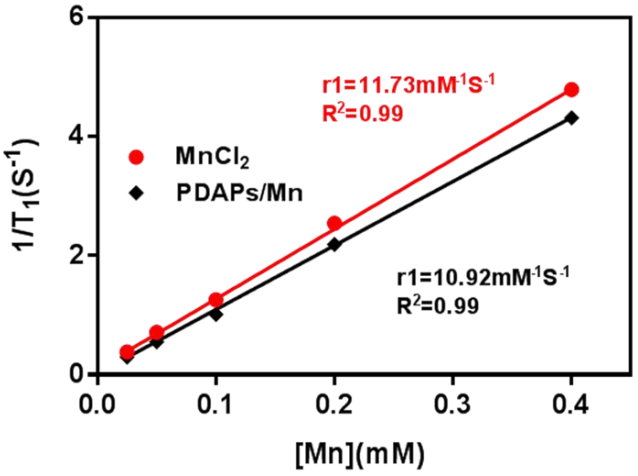

Fig. S8. T_1 relaxation rates of $MnCl_2$ and PDAPs/Mn.

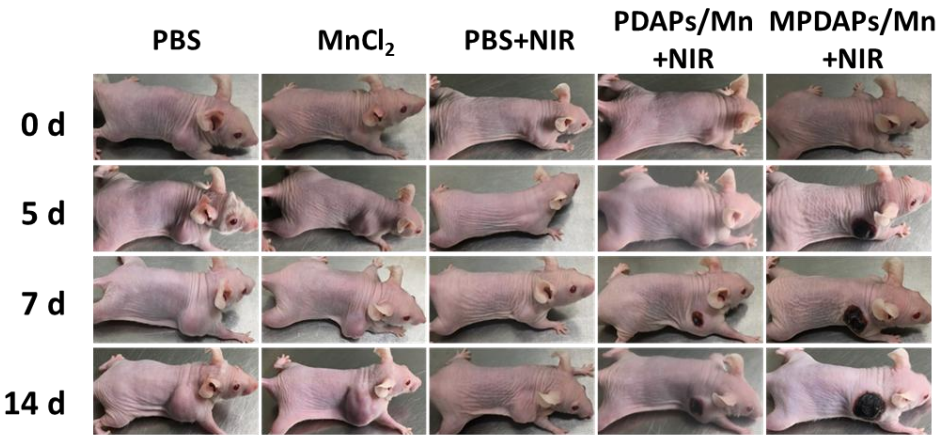

Fig. S9. Digital images of HeLa tumor-bearing mice treated with PBS, $MnCl_2$, PBS + NIR, PDAPs/Mn + NIR and MPDAPs/Mn + NIR at different time points during the treatment.

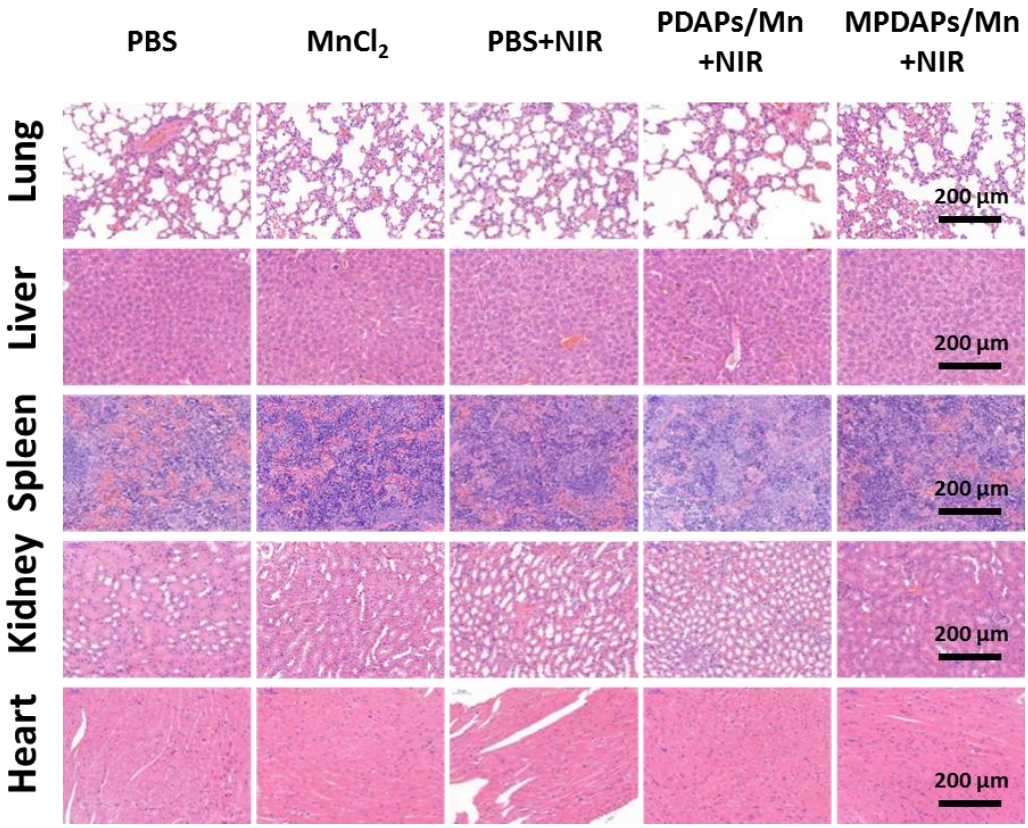

Fig. S10. H&E staining images of major organs (lung, liver, spleen, kidney and heart) that were extracted from the mice after 14 days' treatment, scale bars: 200 μm.

References

1. C. Dai, S. Zhang, Z. Liu, R. Wu and Y. Chen, *ACS Nano.,* 2017, **11**, 9467-94805.
2. G. Shu, H. Wang and X. Zhang, *ACS Appl. Mater. Interfaces,* 2019, **11**, 3323-3333.